J. Comput. Appl. Res. Mech. Eng. Vol. 11. No. 2, pp. 365-379, 2022 *DOI: 10.22061/JCARME.2019.5416.1674*

Journal of Computational and Applied Research in Mechanical Engineering

jcarme.sru.ac.ir

SRTTU

JCARME

ISSN: 2228-7922

Research paper

Thermomechanical behaviour of functionally graded plates with HSDT

B. Sidda Reddy[a,*] and K. Vijaya Kumar Reddy[b]

[a]*Department of Mech. Eng., Rajeev Gandhi Memorial College of Engineering and Technology, Nandyal, Kurnool (Dt), Andhra Pradesh, India-518 501*
[b]*Department of Mech. Eng., JNTUH, Telangana, India-500085*

Article info:

Article history:

Received: 04/06/2019
Accepted: 17/08/2019
Revised: 22/08/2019
Online: 25/08/2019

Keywords:

Functionally graded plates,
Power law distribution,
Navier's Method,
Principle of virtual work,
HSDT,
Thermo-mechanical loading.

***Corresponding author:**
bsrrgmcet@gmail.com

Abstract

This paper presents closed-form formulations of higher order shear deformation theory (HSDT) to analyse the functionally graded plates (FGPs) acted upon a thermo-mechanical load for simply supported (SS) conditions. This theory assumes nullity conditions for transverse stress on bottom and top face of the FGPs. Moreover, it considers the influence of both stresses and strains in the axial and transversal direction. In these improvements, an accurate parabolic variation is assumed in the thickness direction for transverse shear strains. Therefore, this theory omits the use of correction factor for accurately estimating the shear stress. The physical properties of the FGPs are considered to change along the thickness using a power law. The equilibrium relations and constraints on all edges are attained by considering the virtual work. Numerical evaluations are attained based on Navier's approach. The exactness and consistency of the developed theory are ascertained with numerical results for deflections and stresses of SS FGPs; and it is deemed that numerical solutions for thermo-mechanical load will utilize as a reference in the future.

1. Introduction

Functionally graded materials (FGMs) are a future engineered material wherein material properties are continually varied through the thickness direction by mixing two different materials. As a result, internal boundaries does not occur and overcomes the stress concentration setup in composite laminates.

FGMs find potential applications in high thermal environments when compared to other engineering materials because of their superior heat-shielding properties. On the other hand, due to heterogeneity of these materials they also pose confronting problems in mechanics like analysing stress variation, free vibration behavior, buckling and fracture response. Thus, FGMs analysis has to consider the mechanical and thermal load, because several applications such as heat shield of the space shuttle have to provide load carrying capability and protection against heat generated while re-entering into the Earth's environment or the wall of a nuclear reactor.

The mathematical modeling of FGM is a great tool to understand the structural performance under thermo-mechanical loading.

In the recent past Carrera et al. [1] analyzed the influence of stretching in the thickness direction in a single-layered and multilayered FG plates and shells. This theory preserves the transverse normal strain. The conclusion of this theory is to consider the influence of normal strain to get meaning for the inclusion of added inplane variables in the classical theories. Talha and Singh [2] developed a finite element method (FEM) formulations using HSDT to analyze the thermomechanical deformation responses of shear deformable FGM plates.

Mantari and Soares [3] considered thickness stretching HSDT with trigonometric shape function to investigate the static behavior of FGPs. However, considering the trigonometric function involves high computational effort. Sidda Reddy et al. [4] investigated the influence of aspect ratios, thickness ratios and modulus ratios and exponent on the natural frequencies of FGPs using HSDT. Mantari and Granados [5] used a novel first shear deformation theory (FSDT) to investigate FGPs. The equilibrium equations for static bending response are developed by utilizing the virtual work. The equilibrium equations are solved through Navier-type solutions. The FSDTs includes the influence of shear deformation in the transverse direction, however, this theory demands a shear correction factor (SCF) to fulfil the nullity conditions at the lower and top side of the plate. This theory is not well-suited, because of complexity in estimating the accurate SCF. In order to alleviate these, HSDT was formulated with higher order terms in displacements through the thickness coordinate based on Taylors Series. ZhanZhao et al. [6] used the FEM to investigate the bending and vibration of trapezoidal plates made with functionally graded materials by reinforcing with graphene nanoplatelets (GPLs). TianK and Jiang [7] adopted hybrid numerical method to research the conduction of heat in FGPs by changing gradient parameters under the exponential heat source load. Moit et al. [8] used the FEM formulations based on HSDT to investigate the nonlinear static response of FGPs and FG shells. Mohammadi et al. [9] developed the HSDT, to analyse the incompressible rectangular FG thick plates. Further, the influence of incompressibility on the static, dynamic and stability behaviour is investigated.

Kadkhodayan [10], Matsunaga [11-12], Xiang [13], Sidda Reddy et al. [14-15] and Suresh Kumar et al. [16] developed many HSDTs. Most of these theories neglect the stress in the transverse direction on the lower and top side of the plate and stretching influence in the thickness direction.

Cho and Oden [17] employed Galerkin approach to examine the thermo-elastic behaviour of FGMs and explained that the use of FGMs shows significant progress in thermal stress.

Sun and Luo [18] considered the temperature responsive properties to study the propagation of wave and transient analysis of infinite length FGPs. Jafari Mehrabadi and Sobhani Aragh [19] used the third order plate theory to present thermo-elastic analysis of two dimensional FG cylindrical shells. The physical properties are assumed to vary with temperature as well as in axial and radial directions.

Recently, Wagih et al. [20] studied the effect of contact with an elastoplastic FG substrate and a rigid spherical indenture with the help of FEM. Slimane Merdaci and HakimaBelghoul [21] investigated rectangular porous thick FGPs by applying higher order theory for bending response.

Attia et al. [22] researched the bending behaviour of temperature dependent FGPs. The FGP rests on an elastic foundation and acted upon a thermo mechanical load. Fahsi et al. [23] presented a simple and 4 variable refined n^{th} order theory considering the influence of shear deformity and analysed the mechanical responses and buckling behaviour under temperature of FG plates lying on elastic foundation. This contains the undetermined integral terms. Chikh et al. [24] analyzed the thermal buckling response of crossply composite plates applying a simple HSDT with four unknowns. This theory introduces undetermined integral terms. El-Haina et al. [25] presented a simple sinusoidal theory considering the influence of shear deformation to investigate the FG thick sandwich for thermal buckling behaviour.

Menasria et al. [26] used a trigonometric based new displacement field which contains four variables for distributing the transverse shear stress. This displacement field includes undetermined integral terms and analysed the response of FG sandwich plates for thermal buckling. They also studied the impact of thickness and aspect ratios, exponent, loading type, and sandwich plate type. Beldjelili et al. [27] used RPT with 4 variables to research the hygro thermomechanical behaviour for bending of sigmoid FGP lying on elastic foundation. Boutaleb et al. [28] investigated the fundamental frequencies of nanosize FGPs considering the quasi 3D theory including the thickness stretching. They also investigated the effect of nonlocal coefficient, the material index, the aspect ratio and the thickness upon length ratio on the dynamic properties of the FG nanoplates.

Boukhlif et al. [29] used a simple quasi-3D higher order theory considering the shear deformation and stretching influence with only four unknowns to research the fundamental frequencies of FGPs resting on elastic foundation. Bouanati et al. [30] used an efficient quasi 3D theory with three unknowns to investigate the vibration analysis and wave propagation of triclinic and orthotropic plate. They divided the displacement in the transversal direction into two parts, i.e. bending and shear to show their effects on total vibration and wave propagation in anisotropic plates. Ait Atmane et al. [31] used an efficient beam theory to research the bending, buckling and vibration of sandwich FG beams with porosity on two parameter elastic foundations considering the thickness stretching effects.

Benahmed et al. [32] provided a simple quasi three dimensional theory considering the hyperbolic function to research the bending and vibration analyses of FGPs rests on 2 parameter elastic foundation considering the thickness stretching influence. This theory involves only 5 unknowns.

Karami et al. [33] gave a quasi 3D theory for analysing the wave dispersion of nano FGPs resting on an elastic foundation under hygrothermal environment. They considered the thickness stretching influence and shear deformation and involved only five unknowns.

Zaoui et al. [34] used new shape function to analyse the fundamental frequencies of FGPs resting on elastic foundations using quasi-3D theory. This theory considers the effects of transverse shear as well as through the thickness stretching. Bouhadra et al [35] developed an improved higher order theory considering the effect of thickness stretching in FGPs. This theory considers the undetermined integral terms in inplane and transverse displacements varies parabolically in the thickness. Younsi et al. [36] proposed 2D and quasi 3D hyperbolic HSDT with undetermined integrals to investigate the bending and vibration of FGPs considering the thickness stretching influence.

Abualnour et al. [37] proposed a new SDT with five unknowns. This theory considers the stretching influence to analyse the vibration of the SS FG plates and involves only five unknowns. The displacement field introduced contains undetermined integral variables.

The goal of the present research is to study the thermomechanical behavior of SS FGPs considering higher order theories considering the non-nullity conditions for transverse stresses at the upper and lower sides of the plate.

The present theory includes the extensibility in the transverse direction to account for the transverse influence. Thus the SCF is omitted. The material properties are graded in the thickness of the plate. The equilibrium relations and boundary conditions of the FGPs are obtained by adopting the virtual work. Navier's solution is attained for FGPs by applying sinusoidal variation of temperature for SS conditions. The findings are compared to other higher order theories available in the open literature to authenticate the exactness of the present theory in estimating the deformations and stresses of FGPs.

2. Theoretical formulation

Fig. 1 represents a FG plate having physical dimensions. The upper side of the plate is made of ceramic and graded to the lower side that contains the metal. The mid plane is considered as the reference.

The FGP properties are considered to vary with the volume fraction (VF) of materials constituents.

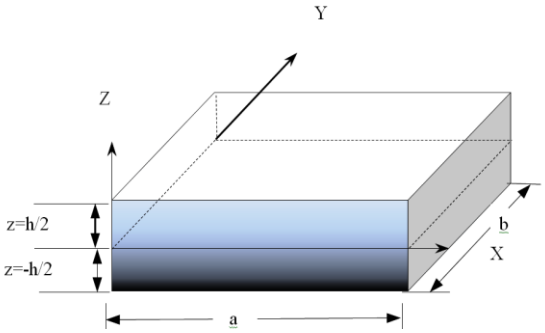

Fig. 1. Representation of FG rectangular plate.

The relation between the physical property of the material and the z coordinate is given as:

$$\varsigma(z) = (\varsigma_t - \varsigma_b)\left(z/h + 0.5\right)^n + \varsigma_b \qquad (1)$$

where ς denotes the effective property of the material, ς_t, and ς_b denotes the physical property respectively on the upper and lower side of the plate and *n* is the material property change parameter. The effective properties of the plate material, such as constant of Elasticity E, density ρ, and constant of rigidity G, change according to Eq. (1); and poisson's ratio (υ) is considered as constant.

2.1. Displacement field

U_1, U_2 and U_3 denote the displacements at any location along x,y and z directions respectively; in the FG plate are expanded in the thickness coordinate using the Taylor's series to obtain the following set of equations. A higher order shear deformation for FGPs used by Sidda Reddy et al [4] are extended to research the thermomechanical behavior of FGPs under simply supported boundary conditions. The displacement functions is expressed as:

$$\left.\begin{aligned} U_1 &= u_m + z\xi_x + z^2 u_m^* + z^3 \xi_x^* \\ U_2 &= v_m + z\xi_y + z^2 v_m^* + z^3 \xi_y^* \\ U_3 &= w_m + z\xi_z + z^2 w_m^* + z^3 \xi_z^* \end{aligned}\right\} \qquad (2)$$

In Eq. (2), the parameters u_m, v_m are the inplane displacements and w_m is the displacement in the transverse direction at the median plane.

ξ_x, ξ_y are rotations about y-axis and x–axis, respectively about median plane.

Similarly u_m^*, v_m^*, w_m^*, ξ_x^*, ξ_y^* and ξ_z^* are the higher order elements defined at the mid-plane.

2.2. Strain-Displacement Equations

The relationship between strains in terms of displacement is given as:

$$\varepsilon_{11} = \varepsilon_{xm} + zk_{xx} + z^2\varepsilon_{xm}^* + z^3 k_{xx}^*$$

$$\varepsilon_{22} = \varepsilon_{ym} + zk_{yy} + z^2\varepsilon_{ym}^* + z^3 k_{yy}^*$$

$$\varepsilon_{33} = \varepsilon_{zm} + zk_{zz} + z^2\varepsilon_{zm}^*$$

$$\gamma_{12} = \varepsilon_{xym} + zk_{xy} + z^2\varepsilon_{xym}^* + z^3 k_{xy}^*$$

$$\gamma_{23} = \phi_{yy} + zK_{yz} + z^2\phi_{yy}^* + z^3 k_{yz}^*$$

$$\gamma_{13} = \phi_{xx} + zK_{xz} + z^2\phi_{xx}^* + z^3 k_{xz}^* \qquad (3)$$

where

$$\varepsilon_{xm} = \frac{\partial u_m}{\partial x};\ \varepsilon_{ym} = \frac{\partial v_m}{\partial y};\ \varepsilon_{zm} = \xi_z;\ k_{xx} = \frac{\partial \xi_x}{\partial x}$$

$$;\ k_{yy} = \frac{\partial \xi_y}{\partial y};\ k_{zz} = 2w_m^*;\ k_{xy}^* = \frac{\partial \xi_x^*}{\partial y} + \frac{\partial \xi_y^*}{\partial x};$$

$$\varepsilon_{xym}^* = \frac{\partial u_m^*}{\partial y} + \frac{\partial v_m^*}{\partial x}$$

$$\varepsilon_{xym} = \frac{\partial u_m}{\partial y} + \frac{\partial v_m}{\partial x},\ k_{xy} = \frac{\partial \xi_x}{\partial y} + \frac{\partial \xi_y}{\partial x},$$

$$\phi_{xx} = \xi_x + \frac{\partial w_m}{\partial x},\ k_{xz} = 2u_m^* + \frac{\partial \xi_z}{\partial x},$$

$$\phi_{xx}^* = 3\xi_x^* + \frac{\partial w_m^*}{\partial x},$$

$$\varepsilon_{xm}^* = \frac{\partial u_m^*}{\partial x},\ \varepsilon_{ym}^* = \frac{\partial v_m^*}{\partial y},\ \varepsilon_{zm}^* = 3\xi_z^*,$$

$$k_{xx}^* = \frac{\partial \xi_x^*}{\partial x},\ k_{yy}^* = \frac{\partial \xi_y^*}{\partial y}$$

$$k^{*}_{xz} = \frac{\partial \xi^{*}_{z}}{\partial x},\ \varepsilon_{xzm} = 2u^{*}_{m} + \frac{\partial \xi_{z}}{\partial y}$$

$$\phi_{yy} = \xi_{y} + \frac{\partial w_{m}}{\partial y},\ \phi^{*}_{yy} = 3\xi^{*}_{y} + \frac{\partial w^{*}_{m}}{\partial y},\ k^{*}_{yz} = \frac{\partial \xi^{*}_{z}}{\partial y},$$

$$\varepsilon_{yzm} = 2v^{*}_{m} + \frac{\partial \xi_{z}}{\partial y} \qquad (4)$$

2.3. Constitutive Relations

The constitutive relations depend on the assumption of $\varepsilon_z \neq 0$, that is thickness stretching is considered. In this case the 3-D model is used. For FGPs the constitutive relations can be expressed as:

$$\begin{aligned}
\sigma_{11} &= Q_{11}(\varepsilon_{11} - \alpha\Delta T) + Q_{12}(\varepsilon_{22} + \varepsilon_{33} - 2\alpha\Delta T)\\
\sigma_{22} &= Q_{11}(\varepsilon_{22} - \alpha\Delta T) + Q_{12}(\varepsilon_{11} + \varepsilon_{33} - 2\alpha\Delta T)\\
\sigma_{33} &= Q_{11}(\varepsilon_{33} - \alpha\Delta T) + Q_{12}(\varepsilon_{11} + \varepsilon_{22} - 2\alpha\Delta T)\\
\tau_{12} &= Q_{44}\,\gamma_{12}\\
\tau_{23} &= Q_{44}\,\gamma_{23}\\
\tau_{13} &= Q_{44}\,\gamma_{13}
\end{aligned} \qquad (5)$$

where $(\sigma_{11}, \sigma_{22}, \sigma_z, \tau_{12}, \tau_{23}, \tau_{13})^t$ and $(\varepsilon_{11}, \varepsilon_{22}, \varepsilon_{33}, \gamma_{12}, \gamma_{23}, \gamma_{13})^t$ are respectively the stresses and strains with reference to the axes, Q_{ij}'s are the elasticity coefficients along the axes of the plate and change along the thickness, as:

$$\begin{aligned}
Q_{11} &= \frac{(1-\upsilon^2)E(z)}{1-3\upsilon^2-2\upsilon^3};\quad Q_{12} = \frac{\upsilon(1+\upsilon)E(z)}{1-3\upsilon^2-2\upsilon^3};\\
Q_{44} &= \frac{E(z)}{2(1+\upsilon)};\\
E(z) &= (E_{ceramic} - E_{metal})\left(\frac{z}{h}+\frac{1}{2}\right)^{n} + E_{metal}\\
\alpha &= (\alpha_{ceramic} - \alpha_{metal})\left(\frac{z}{h}+\frac{1}{2}\right)^{n} + \alpha_{metal}
\end{aligned} \qquad (6)$$

where $E_{ceramic}$ and E_{metal} are the elastic constants of the ceramic and metallic phase respectively, α is thermal expansion co-efficient. ΔT is the temperature raise from a reference. The superscript *t* denotes the transpose of a matrix. If $\varepsilon_{33}=0$, then the plane-stress case is used

$$\begin{aligned}
\sigma_{11} &= Q_{11}(\varepsilon_{11} - \alpha\Delta T) + Q_{12}(\varepsilon_{22} - 2\alpha\Delta T)\\
\sigma_{22} &= Q_{11}(\varepsilon_{22} - \alpha\Delta T) + Q_{12}(\varepsilon_{11} - 2\alpha\Delta T)\\
\tau_{12} &= Q_{44}\,\gamma_{12}\\
\tau_{23} &= Q_{44}\,\gamma_{23}\\
\tau_{13} &= Q_{44}\,\gamma_{13}
\end{aligned} \qquad (7)$$

$$\begin{aligned}
Q_{11} &= Q_{22} = \frac{E(Z)}{1-\upsilon^2} = \frac{(E_c - E_m)\left(\frac{z}{h}+\frac{1}{2}\right)^{n} + E_m}{1-\upsilon^2}\\
Q_{12} &= \upsilon Q_{11}\\
Q_{44} &= \frac{(1-\upsilon^2)}{2(1+\upsilon)}Q_{11}
\end{aligned} \qquad (8)$$

2.4. Equilibrium Equations

The equilibrium equations are obtained by considering the Hamilton's theory and can be given as:

$$0 = \int_{0}^{T} (\delta U + \delta V)\, dt \qquad (9)$$

where

$$\delta U = \int_{A}\left\{\int_{-h/2}^{h/2}\left[\begin{aligned}&\sigma_{11}\delta\varepsilon_{11} + \sigma_{22}\delta\varepsilon_{22} + \sigma_{33}\delta\varepsilon_{33}\\ &+ \tau_{12}\delta\gamma_{12} + \tau_{13}\delta\gamma_{13} + \tau_{23}\delta\gamma_{23}\end{aligned}\right]dz\right\}dx\,dy \qquad (10)$$

$$\delta V = -\int q\delta U_3^{*}\, dx\, dy \qquad (11)$$

where $U_3^{*} = w_m + \frac{h}{2}\xi_z + \frac{h^2}{4}w_m^{*} + \frac{h^3}{8}\xi_z^{*}$ is the deformation in the transverse direction at any location at the upper side of the plate and q is the double sinusoidal load applied at the upper side of the plate.

By substituting Eq. (10-11) in Eq. (9) and integrating in the thickness direction and employing the integration by parts and grouping the coefficients of:

$\delta u_m, \delta v_m, \delta w_m, \delta \xi_x, \delta \xi_y, \delta \xi_z, \delta u_m^*, \delta v_m^* \delta w_m^*, \delta \xi_x^*, \delta \xi_y^*, \delta \xi_z^*$

the equilibrium equations are obtained.

$$\delta u_m : \frac{\partial N_{xx}}{\partial x} + \frac{\partial N_{xy}}{\partial y} = 0$$

$$\delta v_m : \frac{\partial N_{yy}}{\partial y} + \frac{\partial N_{xy}}{\partial x} = 0$$

$$\delta w_m : \frac{\partial Q_{xx}}{\partial x} + \frac{\partial Q_{yy}}{\partial y} + q = 0$$

$$\delta \xi_x : \frac{\partial M_{xx}}{\partial x} + \frac{\partial M_{xy}}{\partial y} - Q_{xx} = 0$$

$$\delta \xi_y : \frac{\partial M_{yy}}{\partial y} + \frac{\partial M_{xy}}{\partial x} - Q_{yy} =$$

$$\delta \xi_z : \frac{\partial S_{xx}}{\partial x} + \frac{\partial S_{yy}}{\partial y} - N_{zz} + \frac{h}{2} q = 0$$

$$\delta u_m^* : \frac{\partial N_{xx}^*}{\partial x} + \frac{\partial N_{xy}^*}{\partial y} - 2S_{xx} = 0$$

$$\delta v_m^* : \frac{\partial N_{yy}^*}{\partial y} + \frac{\partial N_{xy}^*}{\partial x} - 2S_{yy} = 0$$

$$\delta w_m^* : \frac{\partial Q_{xx}^*}{\partial x} + \frac{\partial Q_{xy}^*}{\partial y} - 2M_{zz} + \frac{h^2}{4} q = 0$$

$$\delta \xi_x^* : \frac{\partial M_{xx}^*}{\partial x} + \frac{\partial M_{xy}^*}{\partial y} - 3Q_x^* = 0$$

$$\delta \xi_y^* : \frac{\partial M_{yt}^*}{\partial y} + \frac{\partial M_{xy}^*}{\partial x} - 3Q_y^* = 0$$

$$\delta \xi_z^* : \frac{\partial S_{xx}}{\partial x} + \frac{\partial S_{yy}}{\partial y} - 3N_{zz}^* + \frac{h^3}{8} q = 0 \qquad (12)$$

where the force and moment resultants are expressed as:

$$\begin{Bmatrix} N_{xx} & | & N_{xx}^* & M_{xx} & | & M_{xx}^* \\ N_{yy} & | & N_{yy}^* & M_{yy} & | & M_{yy}^* \\ N_{zz} & | & N_{zz}^* & M_{zz} & | & 0 \\ N_{xy} & | & N_{xy}^* & M_{xy} & | & M_{xy}^* \end{Bmatrix}$$

$$= \int_{-h/2}^{h/2} \begin{Bmatrix} \sigma_{11} \\ \sigma_{22} \\ \sigma_{33} \\ \tau_{12} \end{Bmatrix} \left[1 \mid z^2 \mid Z \mid Z^3\right] dz$$

$$= \int_{-h/2}^{h/2} \begin{bmatrix} Q_{11} & Q_{12} & Q_{12} & 0 \\ Q_{12} & Q_{11} & Q_{12} & 0 \\ Q_{13} & Q_{12} & Q_{11} & 0 \\ 0 & 0 & 0 & Q_{44} \end{bmatrix} \begin{Bmatrix} \varepsilon_{11} \\ \varepsilon_{22} \\ \varepsilon_{33} \\ \gamma_{12} \end{Bmatrix} \left[1 \mid z^2 \mid Z \mid Z^3\right] dz$$

$$- \begin{Bmatrix} N_{xT} & | & N_{xT}^* & M_{xT} & | & M_{xT}^* \\ N_{yT} & | & N_{yT}^* & M_{yT} & | & M_{yT}^* \\ N_{zT} & | & N_{zT}^* & M_{zT} & | & 0 \\ N_{xyT} & | & N_{xyT}^* & M_{xyT} & | & M_{xyT}^* \end{Bmatrix} \qquad (13)$$

$$\begin{Bmatrix} Q_{xx} & | & Q_{xx}^* & S_{xx} & | & S_{xx}^* \\ Q_{yy} & | & Q_{yy}^* & S_{yy} & | & S_{yy}^* \end{Bmatrix} \qquad (14)$$

$$= \int_{-h/2}^{h/2} \begin{Bmatrix} \tau_{13} \\ \tau_{23} \end{Bmatrix} \left[1 \mid Z^2 \mid Z \mid Z^3\right] dz$$

Resultants of thermal forces are given by:

$$\begin{Bmatrix} N_{xT} & | & N_{xT}^* & M_{xT} & | & M_{xT}^* \\ N_{yT} & | & N_{yT}^* & M_{yT} & | & M_{yT}^* \\ N_{zT} & | & N_{zT}^* & M_{zT} & | & 0 \\ N_{xyT} & | & N_{xyT}^* & M_{xyT} & | & M_{xyT}^* \end{Bmatrix}$$

$$= \int_{-h/2}^{h/2} \begin{bmatrix} Q_{11} & Q_{12} & Q_{13} & 0 \\ Q_{12} & Q_{22} & Q_{23} & 0 \\ Q_{13} & Q_{23} & Q_{33} & 0 \\ 0 & 0 & 0 & Q_{44} \end{bmatrix} \begin{Bmatrix} 1 \\ 1 \\ 1 \\ 0 \end{Bmatrix} \alpha \Delta T \left[1 \mid z^2 \mid Z \mid Z^3\right] dz \qquad (15)$$

3. Analysis of FGPs

We are concernedabout the analytical solutions of the Eq. (13-15) for SS FGPs. The following are the expressions to satisfy the SS conditions:

$$[u_m \quad \xi_x \quad u_m^* \quad \xi_x^*]$$
$$= [U_{11}, X_{11}, U_{11}^*, X_{11}^*] \cos(\pi x / a) \sin(\pi y / b)$$
$$[v_m \quad \xi_y \quad v_m^* \quad \xi_y^*]$$
$$= [V_{11}, Y_{11}, V_{11}^*, V_{11}^*] \sin(\pi x / a) \cos(\pi y / b)$$
$$[w_m \quad \xi_z \quad w_m^* \quad \xi_z^*]$$
$$= [W_{11}, Z_{11}, W_{11}^*, Z_{11}^*] \sin(\pi x / a) \sin(\pi y / b) \qquad (16)$$

where $x \in 0, a$ & $y \in 0, b$;

Substituting Eq. (16) in to Eq. (12), and grouping the coefficients, the following matrix in terms of the unknown variables U_{11}, V_{11}, W_{11}, X_{11}, Y_{11}, Z_{11} U_{11}^*, V_{11}^*, W_{11}^*, X_{11}^*, Y_{11}^*, Z_{11}^* are obtained.

$$[X]_{12\times12}[\Delta]_{12\times1}=[F]_{12\times1}$$

Where [X] represents stiffness matrix and Δ is the unknown variables and [F] indicates the force matrix.

4. Results and discussion

In this part some examples are considered and compared with the published studies in the literature to verify the exactness of the present HSDT in estimating the deformations and stresses. The distributions of the deformations and stress of SS FGPs subjected to mechanical, thermal/thermomechanical load are investigated in detail. The properties of the FGPs are

$E_{metal}= 70\times10^9$ Pa,
$E_{ceramic}= 380\times10^9$ Pa, , and $\upsilon= 0.3$

The displacement u and shear stress τ_{xz} are evaluated at (0, b/2), while displacement v and shear stress τ_{yz} are evaluated at (a/2, 0), and the shear stress τ_{xy} is evaluated at (0, 0). The normal stresses σ_x, σ_y, σ_z and the displacement w are evaluated at (a/2, b/2).
For the mechanical/thermal loadings, the plates are subjected to the bisiusoidal normal pressure/temperature of amplitude

$$(q,\Delta T) == (q_{11},T_{11})\,sin(\pi x/a)\,sin(\pi y/b)$$

on the upper side.
The transverse displacements U_3 and the transverse shear stress τ_{13} for mechanical loading are shown in the non-dimensionalized quantities as:

$$\hat{w}=\frac{U_3\times E_{ceramic}}{q\times h} \text{ and } \hat{\tau}_{xz}=\frac{\tau_{13}}{q}$$

All the numerical results for thermal loading are given in the nondimensionalized form as follows:

$$(\hat{u},\hat{v},\hat{w})=(U_1,U_2,U_3)/(\alpha_c T_{mn} h),$$
$$(\hat{\sigma}_x,\hat{\sigma}_y,\hat{\sigma}_z,\hat{\tau}_{xy},\hat{\tau}_{yz},\hat{\tau}_{xz})$$
$$=(\sigma_{11},\sigma_{22},\sigma_{33},\tau_{12},\tau_{23},\tau_{13})/(\alpha_c T_{mn} E_c)$$

For the thermo-mechanical loadings, the plates are subjected to bisinusoidal temperature as well as the pressure on the upper side.
All the numerical results for thermo-mechanical loadings are shown in the nondimensionalized quantities as follows:

$$(\hat{u},\hat{v},\hat{w})=(U_1,U_2,U_3)/h$$
$$(\hat{\sigma}_x,\hat{\sigma}_y,\hat{\sigma}_z,\hat{\tau}_{xy},\hat{\tau}_{yz},\hat{\tau}_{xz})$$
$$=(\sigma_{11},\sigma_{22},\sigma_{33},\tau_{12},\tau_{23},\tau_{13})h^2/a^2q$$

Example 1: In this example, SS FG material plates made of Al/Al_2O_3 are considered. The FGP is acted upon a bisinusoidal pressure load applied at the upper side of the plate. The results predicted by the present HSDT for transverse displacements w and τ_{xz} considering $\varepsilon_{33}=0$ and $\varepsilon_{33}\neq0$ are reported in Table 1. The present theory evaluations are compared to the evaluations of Matsunaga [12] who considered $\varepsilon_{33}\neq0$.
The displacements w and transverse shear stress τ_{xz} predicted by present HSDT with $\varepsilon_{33}\neq0$ are well agreed with the results of Matsunaga [12]. From the present theory it can be noticed that the values of transverse displacements and shear stress τ_{13} considering $\varepsilon_{33}=0$ are larger than those considering $\varepsilon_{33}\neq0$ and the differences decrease with the decrease of thickness of the plane. This is due to the fact that the thick FG plates stretch more along the thickness. Comparing with the results of Matsunaga [12], the difference is ranged from 0.003279% to 0.362138% for transverse displacements and 0.017872 to 7.8246% for transverse shear stress τ_{xz} when $\varepsilon_z\neq0$ is considered.
Example 2: In this example, the sinusoidal variation of the temperature is applied on the upper side of the simply supported FGPs. The results predicted by the present HSDT for inplane displacement u and normal stress σ_z

considering $\varepsilon_{33}=0$ and $\varepsilon_{33}\neq 0$ is presented in Table 2. The present theory evaluations are compared to the evaluations of Matsunaga [12]. It is noticed that, the present results for *u* and stress σ_z are in good agreement with Matsnaga [12] under thermal loading as well. Table 3 shows the comparison of solutions of isotropic plates subjected to thermal loading. The considered thickness ratios a/h are 2, 5, 10, 20 and 100. The *u* and σ_z results are evaluated using zero and non-zero ε_z strain and are compared with the solutions of Matsunaga [12]. The results showed good agreement when $\varepsilon_{33}\neq 0$ is considered.

This research concludes that the influence of stretching has a great influence on the bending behavior of FGPs under both mechanical and thermal loading as $\varepsilon_{33}\neq 0$ gives very close agreement with the published studies in the literature.

4.1. Behavior of FGM plate with thermal load

Functionally graded material structures find potential applications in high thermal environments due to high endurance to temperature gradients, ability to survive to high loads and temperature. In this problem, the response of FGM plate with thermal load is investigated using higher order theory.

Figs. 2-3 show the distribution of $\hat{u}$ and $\hat{w}$ respectively of SS square FGP made with Al/Al_2O_3 against exponent for several values of a/h under thermal load. From the figures it is observed that, the plate is upward deflection since the thermal load acts at the top surface of the plate. The absolute values of inplane displacement increase as exponent(n) increase, while transverse displacement increases within the range of n=0 to n=2 and then decreases. This is due to the reason that, the magnitude of the three dimensional elastic constants Q_{ij} increases up to n=2 and then decreases. Also noted that, the increase of *a/h* decreases the bending stiffness and results in an increase of $\hat{u}$.

The distribution of nondimensionalized inplane and transverse displacements $\hat{u}$ and $\hat{w}$ along the thickness using a present HSDT of SS square Al/Al_2O_3 FGPs under sinusoidal temperature for different values of exponent *n* and *a/h=10* are shown in Figs. 4-5. The variation of dimensionless normal and shear stresses across the thickness direction for different values of exponent *n* and *a/h=10* are shown in Figs. 6-11. From the figures, it is noted that the nondimensionalized normal stresses $\hat{\sigma}_x$ and $\hat{\sigma}_y$ are tensile at the top and bottom surface of the plate when n=10 and compressive throughout the plate when n=0, 0.5 and 1. However, at n=4, the stresses are tensile at the upper surface of the plate and compressive at the lower surface of the plate under sinusoidal temperature. The nondimensionalized normal stress $\hat{\sigma}_z$ is tensile for n=0, 1, 4, 10 and compressive for n=0. 5 at the lower and upper side of the plate. It is also noteworthy to observe that the normal stresses $\hat{\sigma}_x$, $\hat{\sigma}_y$ and $\hat{\sigma}_z$ are the same at different points above and below the mid-plane when n=10. As exhibited in Fig. 9, the $\hat{\tau}_{xy}$ is compressive throughout the plate for all values of exponent *n*. But in Fig. 10 it is seen that the transverse shear stress $\hat{\tau}_{yz}$ is tensile at the upper surface of the plate and compressive at the lower side of the plate for n=0, 1, 4 and at n=0.5 and 10 it is tensile.

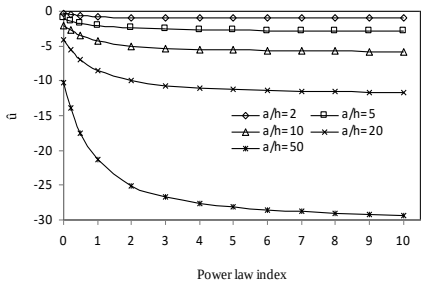

Fig. 2. Influence of exponent on nondimensionalized in-plane displacement ($\hat{u}$) for SS FGPs (a/h=2, 5, 10, 20, 50) under thermal load.

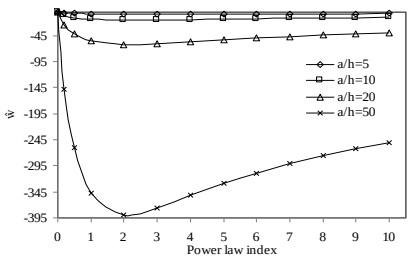

Fig. 3. Influence of exponent on nondimensionalized transverse displacement ($\hat{w}$) for SS FGPs (a/h=5, 10, 20, 50) under thermal load.

Table 1. Comparison of solutions of FG plates under sinusoidal pressures.

a/h	n		Presen $\varepsilon_{33}=0$ (1)	Present $\varepsilon_{33}\neq 0$ (2)	Matsunaga [12] (3)	%Error between (1) & (3)	%Error between (2) & (3)
5	0	$\hat{w}$	21.4575	20.9866	20.98	2.225329	0.031449
		$\hat{\tau}_{xz}$	1.18735	1.1869	1.186	0.113699	0.075828
	0.5	$\hat{w}$	32.3549	31.9001	31.8	1.715042	0.313792
		$\hat{\tau}_{xz}$	1.21301	1.21335	1.217	0.32893	0.30082
	1	$\hat{w}$	41.816	41.3951	41.39	1.018749	0.01232
		$\hat{\tau}_{xz}$	1.18719	1.18848	1.184	0.268702	0.376952
	4	$\hat{w}$	65.2529	65.013	65.0	0.387569	0.019996
		$\hat{\tau}_{xz}$	1.0005	1.00507	1.073	7.24638	6.75873
	10	$\hat{w}$	76.7671	76.2425	76.24	0.686622	0.003279
		$\hat{\tau}_{xz}$	1.07547	1.08084	1.078	0.23525	0.262759
10	0	$\hat{w}$	296.058	294.254	294.3	0.593803	0.01563
		$\hat{\tau}_{xz}$	2.38413	2.38398	2.383	0.047397	0.041108
	0.5	$\hat{w}$	453.716	452.037	450.4	0.730854	0.362138
		$\hat{\tau}_{xz}$	2.43518	2.43545	2.435	0.007392	0.018477
	1	$\hat{w}$	589.03	587.536	587.5	0.259749	0.006127
		$\hat{\tau}_{xz}$	2.38405	2.38482	2.383	0.044043	0.076316
	4	$\hat{w}$	882.341	881.67	881.7	0.072648	0.0034
		$\hat{\tau}_{xz}$	2.01285	2.01531	2.173	7.95638	7.8246
	10	$\hat{w}$	1008.92	1007.18	1007	0.190303	0.017872
		$\hat{\tau}_{xz}$	2.16235	2.16514	2.166	0.1688	0.03972

Table 2. Comparison of solutions of FG plates subjected to temperature.

		Source	Power law index (n)				
a/h			0	0.5	1	4	10
5	$\bar{u}$	$\varepsilon_{33}=0$	-1.0345	-1.7451	-2.1249	-2.774	-2.9478
		$\varepsilon_{33}\neq 0$	-1.00194	-1.69596	-2.06859	-2.68538	-2.83659
		Matsunaga [12]	-1.003	-1.696	-2.069	-2.689	-2.840
	$\bar{\sigma}_z$	$\varepsilon_z\neq 0$	-0.00184	-0.00819	-0.00276	0.0262	0.0727
		Matsunaga [12]	-0.002227	0.1439	0.1518	0.1277	0.1016
10	$\bar{u}$	$\varepsilon_{33}=0$	-2.069	-3.4948	-4.2499	-5.5287	-5.8751
		$\varepsilon_{33}\neq 0$	-2.05218	-3.46939	-4.22056	-5.48239	-5.81735
		Matsunaga [12]	-2.052	-3.469	-4.221	-5.483	-5.818
	$\bar{\sigma}_z$	$\varepsilon_{33}\neq 0$	-0.000117	-0.008447	-0.000346	0.0326621	0.078631
		Matsunaga [12]	-0.0001435	0.03647	0.03835	0.03233	0.02689

Table 3. Comparison of solutions of isotropic plates subjected to thermal load.

a/h	$\hat{u}$			$\hat{\sigma}_z$	
	$\varepsilon_{33}=0$	$\varepsilon_{33}\neq 0$	Matsunaga [12]	$\varepsilon_{33}\neq 0$	Matsunaga [12]
2	-0.413803	-0.350716	-0.3595	-0.0612457	-0.06993
5	-1.03451	-1.00194	-1.003	-0.00184404	-0.002229
10	-2.06902	-2.05218	-2.052	-0.000117656	-0.0001435
20	-4.13803	-4.12955	-4.130	-7.39065×10^{-6}	-0.000009037
100	-20.6902	-20.6885	-20.69	-1.1844×10^{-8}	-1.449×10^{-6}

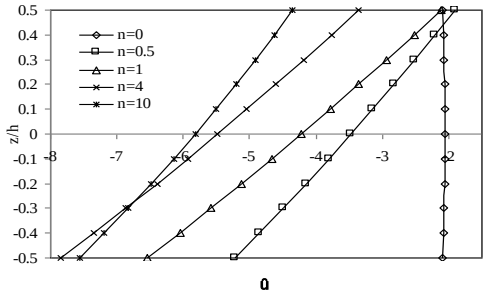

Fig. 4. Distribution of $\hat{u}$ along the thickness (z/h) of SS FGM plates subjected to sinusoidal temperature (a/h=10).

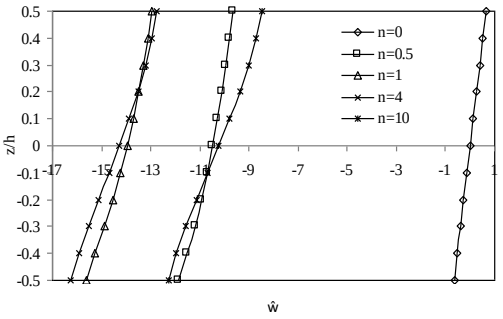

Fig. 5. Distribution of $\hat{w}$ along the z/h of SS FGPs acted upon a sinusoidal temperature (a/h=10).

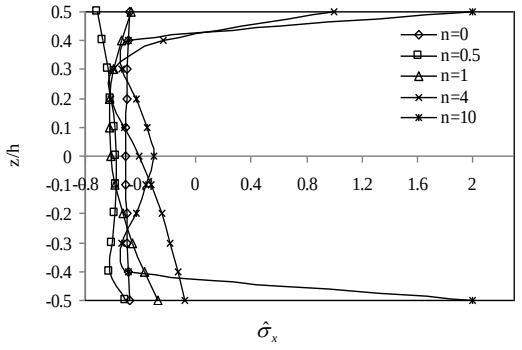

Fig. 6. Distribution of $\hat{\sigma}_x$ along z/h of SS FGM plates acted upon a sinusoidal temperature (a/h=10).

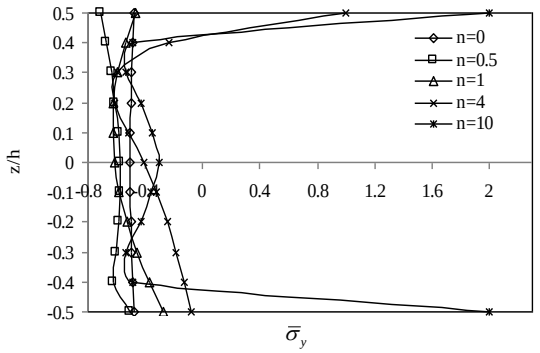

Fig. 7. Distribution of $\hat{\sigma}_y$ along z/h of SS FGM plates acted upon a sinusoidal temperature (a/h=10).

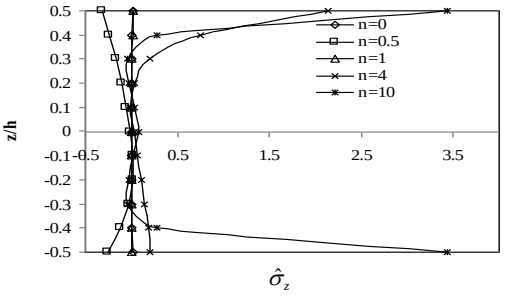

Fig. 8. Distribution of $\hat{\sigma}_z$ along z/h of SS FGM plates acted upon a sinusoidal temperature (a/h=10).

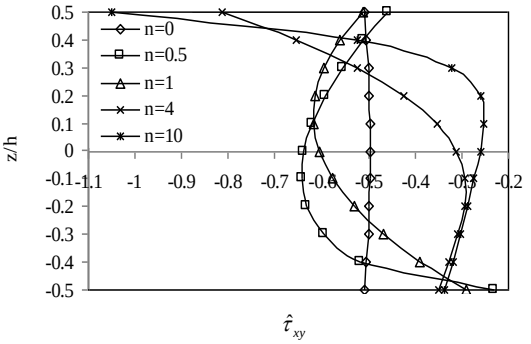

Fig. 9. Distribution of $\hat{\tau}_{xy}$ along z/h of SS FGM plates subjected to sinusoidal temperature for different values of exponent (a/h=10).

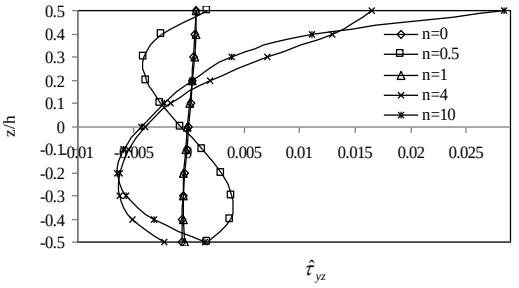

Fig. 10. Distribution of $\hat{\tau}_{yz}$ along z/h of SS FGM plates subjected to sinusoidal temperature for different values of exponent (a/h=10).

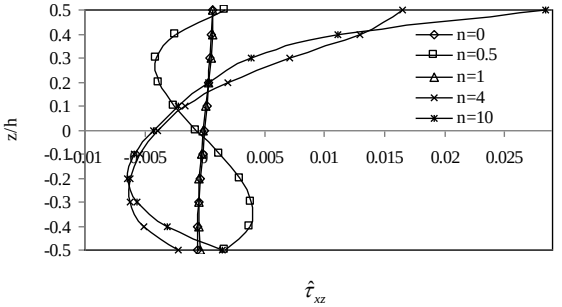

Fig. 11. Distribution of $\hat{\tau}_{xz}$ along z/h of simply supported FGM plates subjected to sinusoidal temperature for different values of exponent (a/h=10).

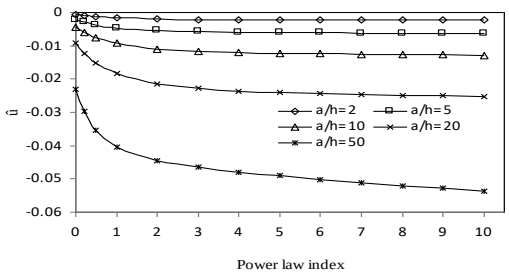

Fig. 12. Influence of *n* on nondimensionalized in-plane displacement ($\hat{u}$) for SS FGPs (a/h=2, 5, 10, 20, 50) under thermo-mechanical load.

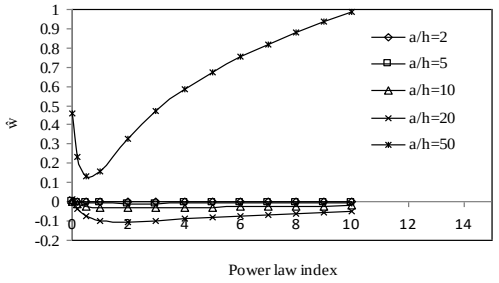

Fig. 13. Influence of *n* on nondimensionalized transverse displacement ($\hat{w}$) for SS FGPs (a/h=2, 5, 10, 20, 50) under thermo-mechanical load.

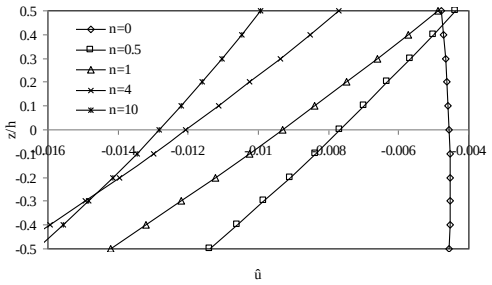

Fig. 14. Distribution of $\hat{u}$ along z/h of SS FGM plates subjected to thermo-mechanical load (a/h=10).

4.2. Behavior of FG plate with thermo-mechanical load

The displacements and stress distributions of SS FG plates under thermomechanical loading is shown through Figs. 12-20. The plate is exposed to a temperature T_{mn} at the top surface =300^{0}C and the mechanical load q_{mn} =1N/mm^2. Figs. 12-13 plots the distribution of nondimensionalized inplane and transverse displacements against exponent for various a/h values. The absolute values of inplane displacement increase with the increase of *n*, while transverse displacement increases within the range of *n*=0 to *n*=2 and then decreases when a/h is less than 50. At a/h 50, the transverse displacements decrease within the range *n*=0 to *n*=0. 5 and then increase.

The distribution of $\hat{u}$ and $\hat{w}$ along the thickness direction using a present HSDT of simply supported square Al/Al_2O_3 FG plates under thermo-mechanical load for several values of *n* and *a/h=10* is shown in Figs. 14-15. The distribution of nondimensionalized normal and shear stresses along thickness direction for several values of *n* and *a/h=10* is depicted in Figs. 16-20. From the Figs. 16-17, it is noted that the nondimensionalized normal stresses $\hat{\sigma}_x$ and $\hat{\sigma}_y$ are tensile at the upper face of the plate and compressive at the lower side of the plate when *n*=4 and 10 and compressive throughout the plate when *n*=0, 0.5 1 and 4. The nondimensionalized normal stress $\hat{\sigma}_z$ is tensile throughout the plate for *n*=0, 1, 4, 10 and compressive throughout at *n*=0.5 as seen in Fig. 18. From Fig. 19, it is seen that the $\hat{\tau}_{xy}$ is compressive throughout the plate for all values *n*. But in Fig. 20 it can be noticed that the transverse shear stress $\hat{\tau}_{yz}$ shows both tensile and compressive behavior for all values of *n*.

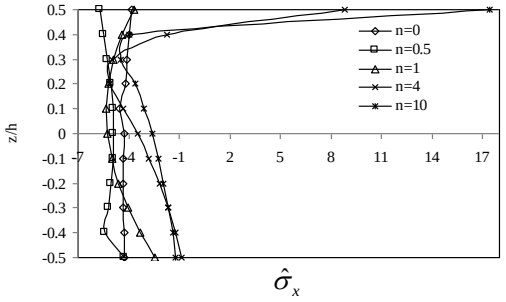

Fig. 16. Distribution of $\hat{\sigma}_x$ along z/h of SS FGM plates subjected to thermo-mechanical load for several values of exponent (a/h=10).

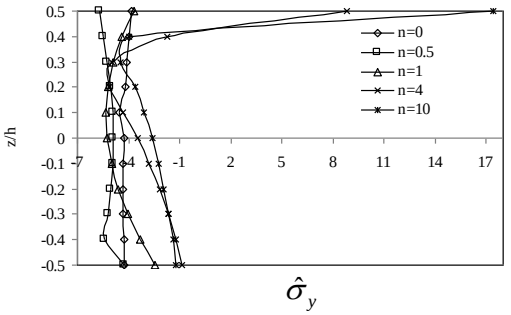

Fig. 17. Distribution of $\hat{\sigma}_y$ along z/h of SS FGM plates subjected to thermo-mechanical load for several values of exponent (a/h=10).

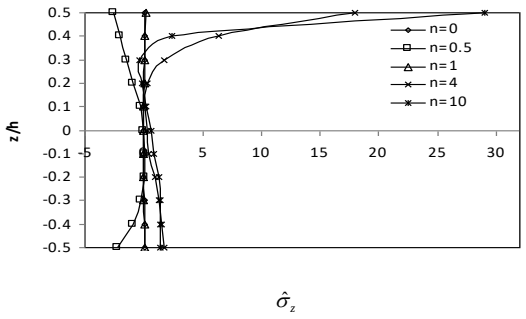

Fig. 18. Variation of nondimensionalized normal stress ($\hat{\sigma}_z$)along z/h of SS FGM plates subjected to thermo-mechanical load (a/h=10).

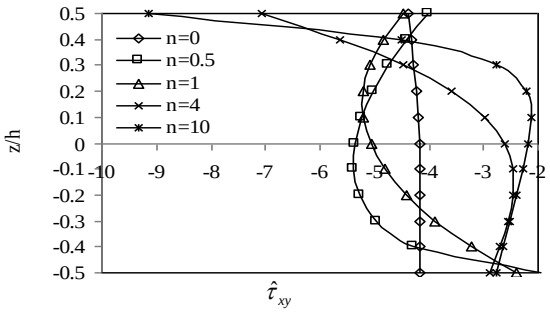

Fig. 19. Distribution of $\hat{\tau}_{xy}$ along z/h of SS FGM plates subjected to thermo-mechanical load (a/h=10).

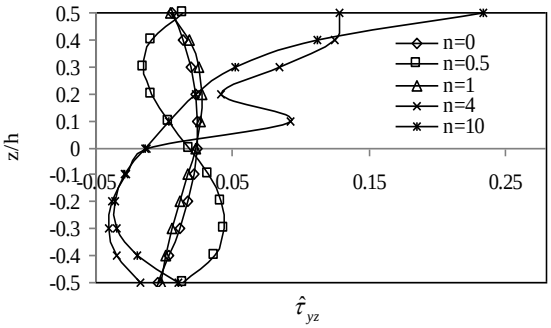

Fig. 20. Distribution of $\hat{\tau}_{yz}$ along z/h of SS FGPs acted upon a thermo-mechanical load (a/h=10).

5. Conclusions

A thickness stretching HSDT has been developed with nonzero transverse stress on the lower face and top face of the SS FG plates to estimate deformations and stress acted upon thermal/ thermomechanical loads.

The numerical results estimated by this theory were compared to published studies in the literature. The results considered with $\varepsilon_{33} \neq 0$ are well-agreed with the published results in the literature.

The distributions of the properties of the material along z/h influence the deformations and stresses in FGPs acted upon a thermal and thermo-mechanical load. The FGPs behavior are not necessarily among those at the corresponding points in isotropic plates.

References

[1] E. Carrera, S. Brischetto and M. Cinefra, "Soave Effects of thickness stretching in functionally graded plates and shells", *Compos Part B: Eng*, Vol. 42, pp.123-133, (2011).

[2] M. Talha and B. N. Singh, "Thermo-mechanical deformation behavior of functionally graded rectangular plates subjected to various boundary conditions and loadings", *Int. J Aerosp. Mech. Eng.*, Vol. 6, No. 1, pp. 14-25, (2012).

[3] J. L. Mantari and C. Guedes Soares, "A novel higher-order shear deformation theory with stretching effect for functionally graded plates", *Compos.: Part B*, Vol. 45, No. 1, pp. 268–281 (2013).

[4] B. Sidda Redddy, J. Suresh Kumar, C. Eswara Reddy and K. Vijaya Kumar Reddy, "Free Vibration Behaviour of Functionally Graded Plates Using Higher-Order Shear Deformation Theory", *J. Appl. Sci. Eng.*, Vol. 17, No. 3, pp. 231-241, (2014).

[5] J. L. Mantari and E. V. Granados, "A refined FSDT for the static analysis of functionally graded sandwich plates", *Thin-Walled Struct.*, Vol. 90, pp. 150-158, (2015).

[6] Z. Zhao, C. Feng, Y. Wang and J. Yang, "Bending and vibration analysis of functionally graded trapezoidal nano-composite plates reinforced with grapheme nano-platelets (GPLs)", *Compos. Struct.*, Vol. 180, No. 15, pp. 799-808, (2017).

[7] J. H. Tian and K. Jiang, "Heat conduction investigation of the functionally graded materials plates with variable gradient parameters under exponential heat source

load", *Int. J. Heat and Mass Transfer*, Vol.122, pp. 22-30, (2018).

[8] J. S. Moita, V. Franco, C. Cristóvão, M. Mota Soares and J. Herskovits, "Higher-order finite element models for the static linear and nonlinear behaviour of functionally graded material plate-shell structures", *Compos. Struct.*, Vol. 212, No. 15, pp. 465-475, (2019).

[9] M. Mohammadi, E. Mohseni and M. Moeinfar, "Bending, buckling and free vibration analysis of incompressible functionally graded plates using higher order shear and normal deformable plate theory", *Appl. Math. Modell.*, Vol. 69, pp. 47-62 (2019).

[10] M. E. Golmakani and M. Kadkhodayan, "Nonlinear bending analysis of annular FGM plates using higher order shear deformation plate theories", *Compos. struct*, Vol. 93, No. 2, pp. 973-982, (2011).

[11] H. Matsunaga, "Free vibration and stability of functionally graded plates according to a 2-D higher-order deformation theory", *Compos. struct*, Vol. 82, No. 4, pp. 499-512, (2008).

[12] H. Matsunaga, "Stress analysis of functionally graded plates subjected to thermal and mechanical loadings, *Compos. struct*, Vol. 87, No. 4, pp. 344-357, (2009).

[13] S. Xiang and G. W. Kang, "A nth-order shear deformation theory for the bending analysis on the functionally graded plates", *Eur. J. Mech. A/Solids*, Vol. 37, pp. 336-343, (2013).

[14] J. Suresh Kumar, B. Sidda Reddy, C. Eswara Reddy and K. Vijaya Kumar Reddy, "Nonlinear Thermal Analysis of Functionally Graded Plates Using Higher Order Theory", *Innovative Syst. Des. Eng.*, Vol. 2 No. 5, pp. 1-13, (2011).

[15] B. Sidda Reddy, J. Suresh Kumar, C. Eswara Reddy and K. Vijaya Kumar Reddy, "Buckling Analysis of Functionally Graded Material Plates Using Higher Order Shear Deformation Theory", *J. Compos.*, Vol. 2013, Article ID 808764, pp.12 pages, (2013).

[16] J. Suresh Kumar, B. Sidda Reddy and C. Eswara Reddy. "Nonlinear bending analysis of functionally graded plates using higher order theory", *Int. J. Eng. Sci.,Technol. (IJEST)*, Vol. 3, No. 4, pp. 3010-3022, (2011).

[17] J. R Cho and J. T. Oden, "Functionally gradient material: a parametric study on thermal stress characteristics using Galerkin scheme", *Compu. Methods Appl. Mech. Eng.*, Vol. 188, No. 1-3, pp. 103-115, (2000).

[18] D. Sun and S. N. Luo "Wave propagation and transient response of a functionally graded material plate under a point impact load in thermal environments", *Appl. Math. Modell.*, Vol. 36, No. 1, pp. 444–462, (2012).

[19] S. Jafari Mehrabadi and B. Sobhani Aragh, "On the thermal analysis of 2-D temperature-dependent functionally graded open cylindrical shell", *Compos. Struct.*, Vol. 96, pp. 773–785, (2013).

[20] A. Wagih, M. A. Attia, A. A. Abdel Rahman, K. Bendine and T. A. Sebaey, "On the indentation of elastoplastic functionally graded materials", *Mech. Mater.*, Vol. 129, pp. 169-188, (2019).

[21] S. Merdaci and H. Belghoul, "High-order shear theory for static analysis of functionally graded plates with porosities, *Comptes Rendus Mécanique*, Vol. 347, No. 3, pp. 207-217, (2019).

[22] A. Attia, A. Anis Bousahla, A. Tounsi, S. R. Mahmoud and A. S. Alwabl, "A refined four variable plate theory for thermoelastic analysis of FGM plates resting on variable elastic foundations", *Struct. Eng. Mech.*, Vol. 65, No. 4, pp.453-464, (2018).

[23] A. Fahsi, A. Tounsi, H. Hebali, A. Chikh, E. A. Adda Bedia and S. R. Mahmoud, "A four variable refined nth-order shear deformation theory for mechanical and thermal buckling analysis of functionally graded plates", *Geomech. Eng.*, Vol. 13, No. 3, pp. 385-410, (2017).

[24] A Chikh, A Tounsi, H. Hebali and S. R. Mahmoud, "Thermal buckling analysis of cross-ply laminated plates using a

simplified HSDT", *Smart Struct. and Syst.*, Vol. 19, No. 3, pp. 289-297, (2017).
[25] F. El-Haina, A. Bakora, A. Anis Bousahla, A. Tounsi and S. R. Mahmoud, "A simple analytical approach for thermal buckling of thick functionally graded sandwich plates", *Struct. Eng. Mech.*, Vol. 63, No. 5, pp. 585-595, (2017).
[26] M. Abderrahmane, B. Abdelhakim, A. Tounsi, A. Anis Bousahla and S. R. Mahmoud, "A new and simple HSDT for thermal stability analysis of FG sandwich plates", *Steel Compos. Struct.*Vo. 25, No. 2, pp.157-175 (2017).
[27] Y. Beldjelili, A. Tounsi and S. R. Mahmoud, "Hygro-thermo-mechanical bending of S-FGM plates resting on variable elastic foundations using a four-variable trigonometric plate theory", *Smart Struct. Syst.*, Vol. 18, No. 4, pp. 755-786, (2016).
[28] S. Boutaleb, K. Halim Benrahou, A. Bakora, A. Algarni, A. Anis Bousahla, A. Tounsi, A. Tounsi and S. R. Mahmoud, "Dynamic analysis of nanosize FG rectangular plates based on simple nonlocal quasi 3D HSDT", *Adv. Nano Res.*, Vol. 7, No. 3, pp.189-206, (2019).
[29] Z. Boukhlif, M. Bouremana, F. Bourada, A. Anis Bousahla, M. Bourada, A. Tounsi and M. A. Al-Osta, "A simple quasi-3D HSDT for the dynamics analysis of FG thick plate on elastic foundation", *Steel Compos. Struct.*, Vol. 31, No. 5, pp. 503-516, (2019).
[30] S. Bouanati, K. Halim Benrahou, H. A. Atmane, S. A. Yahia, F. Bernard, A. Tounsi and E. A. Adda Bedia, "Investigation of wave propagation in anisotropic plates via quasi 3D HSDT", *Geomech. Eng.*, Vol. 18, No. 1, pp. 85-96, (2019).
[31] H. A. Atmane, A. Tounsi and F. Bernard, "Effect of thickness stretching and porosity on mechanical response of a functionally graded beams resting on elastic foundations". *Int. J. Mech. Mater. Des*. Vol. 13, No. 1, pp. 71-84, (2017).
[32] A. Benahmed, M. S. Ahmed Houari, S. Benyoucef, K. Belakhdar and A. Tounsi, "A novel quasi-3D hyperbolic shear deformation theory for functionally graded thick rectangular plates on elastic foundation", *Geomech. Eng.*, Vol. 12, No. 1, pp. 9-34, (2017).
[33] B. Karami, M. Janghorban, D. Shahsavari and A. Tounsi, "A size-dependent quasi-3D model for wave dispersion analysis of FG nanoplates", *Steel Compos. Struct.*, Vol. 28, No. 1, pp. 99-110, (2018).
[34] F. Z. Zaoui, O. Djamel and A. Tounsi, "New 2D and quasi-3D shear deformation theories for free vibration of functionally graded plates on elastic foundations", *Compos. Part B Eng.*, Vol.159, pp. 231-247 (2019).
[35] A. Bouhadra, A. Tounsi, A. Anis Bousahla, S. Benyoucef and S. R. Mahmoud, "Improved HSDT accounting for effect of thickness stretching in advanced composite plates", *Struct. Eng. Mech.*, Vol. 66, No. 1, pp. 61-73 (2018).
[36] A. Younsi, A. Tounsi, F. Z. Zaoui, A. Anis Bousahla and S. R. Mahmoud, "Novel quasi-3D and 2D shear deformation theories for bending and free vibration analysis of FGM plates", *Geomech. Eng.*, Vol. 14, No. 6, pp. 519-532, (2018).
[37] M. Abualnour, M. S. A. Houari, A. Tounsi, E. A. A. Bedia and S. R. Mahmoud, "A novel quasi-3D trigonometric plate theory for free vibration analysis of advanced composite plates", *Compos. Struct.*, Vol. 184, pp. 688-697, (2018).

How to cite this paper:

B. Sidda Reddy and K. Vijaya Kumar Reddy, "Thermomechanical behaviour of Functionally Graded Plates with HSDT,", *J. Comput. Appl. Res. Mech. Eng.*, Vol. 11, No. 2, pp. 365-379, (2022).

DOI: 10.22061/JCARME.2019.5416.1674

URL: https://jcarme.sru.ac.ir/?_action=showPDF&article=1121